Surface & Coatings Technology 358 (2019) 409–415

Contents lists available at ScienceDirect

Surface & Coatings Technology

journal homepage: www.elsevier.com/locate/surfcoat

Electroless carbon fibers: A new route for improving mechanical property and wettability of composites

Yuanlin Xue[a], Wenge Chen[a,*], Qian Zhao[a], YongQing Fu[b,*]

[a] School of Materials Science and Engineering, Xi'an University of Technology, Shaanxi, Xi'an 710048, PR China
[b] Faculty of Engineering and Environment, Northumbria University, Newcastle upon Tyne NE1 8ST, UK

ARTICLE INFO

Keywords:
Carbon fiber
Electroless plating
Fracture strength
Wettability

ABSTRACT

For carbon fiber reinforced metal matrix composites, there are many potential problems such as severe agglomeration of carbon fibers (CFs), their poor interfacial wettability with the matrix, and poor mechanical strength. To solve these problems, we proposed to use electroless plating to coat a layer of Ni onto the CFs, and then studied their interfacial structures, fracture strain/strength and wettability. The coated Ni layer was uniformly distributed onto and well bonded with the CFs. The maximum strain of the CFs coated with the Ni layer was increased by 23.4%, though their average fracture strength was slightly decreased from 3.5 GPa to 2.25 GPa. The wettability of the Ni-coated fiber was significantly improved, verified from testing results using both a dip coating method and a fiber reinforced composite simulation test.

1. Introduction

Carbon fiber (CF) is a microcrystalline carbon material, containing more than 92 wt% of carbon [1]. It has high axial strength, low density (e.g., 1/4 of steel's density and 1/2 of aluminum alloy's density), light weight, high fracture strength (2–7 GPa), high tensile modulus (200–500 GPa), good conductivity (5–17 μΩ·m) and low thermal expansion coefficient (0–1.1 × 10^{-6} K^{-1}) [2–4]. For these reasons, the CFs are often used as the reinforcement agents in synthesis of metal matrix composites [1,5–9]. As-received and untreated CFs normally have relatively smooth surfaces, low surface energy, low reactivity (e.g., lack of chemically active functional groups), poor chemical stability with certain metals such as iron, poor interfacial wettability and poor interfacial adhesion, all of which significantly affect the mechanical properties of composites and restrict their wide-range applications [10]. Therefore, it is critical to modify the surfaces of the CFs to solve the above problems. Coating the surfaces of CFs with a metallic layer is one of the potential solutions. This method not only solves the problems of severe agglomeration of the CFs and their poor interfacial wettability with the matrix, but also avoids the significant reaction of the CFs with metals such as iron [11,12]. Metal coated CFs can also be combined with non-metallic materials such as resin, rubber and plastics in order to fabricate new types of non-metal matrix composites with excellent permeability, conductivity and thermal conductivity. For example, Lv et al. [13] prepared Ni-coated CFs using a continuous electroplating method, and the Ni-layer was well adhered to the CFs. Both the conductivity and oxidation resistance of the Ni coated CFs were improved. The electrical resistivity was decreased to 0.74 × 10^{-6} Ω·m, and the initial oxidation temperature of the Ni coated CFs was ~100 °C higher than that of the untreated CFs. Halouzk et al. [14] electroplated a nanoscale copper layer onto the surfaces of CFs, and this process was performed in the ultra-pure water, thus the contamination of Cu layer during the preparation process was minimized. Wan et al. [15,16] prepared FeCo coated and FeCo/CuO double-layer coated CFs using an electro-deposition method. Results showed that both dielectric and magnetic losses have been decreased when using the CFs coated with the FeCo/CuO double layer because of its double-layer structure, thus improving permittivity and providing good absorption properties. Karim et al. [17] electro-deposited spherical Fe_3O_4 particles (with an average particle size of 50 μm) onto the CFs at 80 °C. Ceng et al. [18] prepared nickel-plated CFs using a wire mesh catalysis method instead of the conventional palladium activation method, and reported that the deposited Ni coating was uniform and compact, although the quality of coating was significantly dependent on the catalytic process. Li et al. [19] used Ni(CO) as a precursor to deposit a continuous and compact nickel layer on the surfaces of CFs using carbonyl metal organic chemical vapor deposition (MOCVD). Their results showed that the film deposited on the surface of CFs was pure nickel with a good adhesion with the CFs. Fracture strength of the CFs was increased by 34.9% and oxidation resistance of the CFs was

* Corresponding authors.
E-mail addresses: wgchen001@263.net (W. Chen), richard.fu@northumbria.ac.uk (Y. Fu).

https://doi.org/10.1016/j.surfcoat.2018.11.072
Received 30 August 2018; Received in revised form 19 November 2018; Accepted 23 November 2018
Available online 24 November 2018

improved effectively. Dyadyura et al. [20] used a spraying technology to coat a titanium layer onto the CFs to obtain good physico-mechanical and tribo-mechanical properties.

Currently various metals such as copper, silver, cobalt, chrome, nickel, titanium and iron [16,21–23] have been coated onto the CFs using various coating processes including physical vapor deposition (PVD), chemical vapor deposition (CVD), sol-gel, electroplating and electroless plating [24–28]. Among these methods, the electroless plating has the advantages of low cost and simple process. Sodium hypophosphite reduced electroless nickel plating is the mostly reported method for the CFs [29,30]. Most researchers are currently focusing their work on process optimization and exploration of new preparation methods for the coated CFs. However, there are few studies focused on fundamental issues, such as the interfacial structures, bonding mechanisms, and surface wettability between the metal layers and CFs, as well as their relationships with mechanical properties of the composite fibers. In this work, we prepared electroless nickel-plated CFs and investigated their interfacial microstructures, tensile properties, fracture mechanism, bonding strength and surface wettability of the composite fibers.

2. Experiment

2.1. Preparation of Ni-coated CFs

Commercial CFs (with their key properties listed in Table 1) were heated to 480 °C and maintained for 60 min to burn out the organic adhesive on their surfaces. They were then soaked in acetone for 60 min, followed by cleaning with de-ionized (DI) water and drying. The treated CFs were heated in a concentrated nitric acid (68 wt%) at 90 °C for 60 min to increase their surface reactivity. They were then washed in a diluted solution of NaOH for neutralization. $SnCl_2$ of 0.3 g was dissolved into 32 mL HCl (38 wt%), and DI water was then added into this solution to form a sensitized liquid of 300 mL. The treated CFs were sensitized for 5 min in the above sensitized liquid, stirred slowly during the sensitization process, and then washed for 2 min with the running water.

Before electroless plating, in order to improve the adhesion of nickel ions, the surfaces of the CFs were activated using palladium ion solution. $PbCl_2$ of 0.3 g was dissolved in 24 mL HCl (38 wt%), and then DI water was added inside to prepare a solution of 300 mL. The sensitized CFs were immersed in the liquid for 5 min to activate their surfaces, and then were immersed in the electroless plating solution (with its key components listed in Table 2). The Ni plating process was performed at 65 °C for 3 min in the alkaline condition (with a pH value of ~8) in order to reduce the content of phosphorus in the coating [31,32]. Finally, the Ni-coated CFs were washed and dried.

2.2. Characterization and performance testing

Crystalline phases of the Ni-coated CFs were analyzed using X-ray diffraction (XRD, 7000 X ray diffractometer, Cu K_α, 40 kV/30 mA, 2θ range: 10°–90°, scanning speed: 0.8–1 °/min and a step size of 0.02°). The coated CFs was spread out onto the substrate, and the residual stress of the fiber was estimated using the XRD results based on the 2θ-$\sin^2(\psi)$ method, during which the incident angles (ψ) were controlled to be 0, 15 and 30°, and the corresponding 2θ values were obtained. Surface morphologies of the CFs before and after electroless plating were characterized using a scanning electron microscope (SEM, TESCAN VEGAIII XMU). Surface composition of the CFs was analyzed using an energy dispersive X-ray spectroscope (EDS) attached with the SEM.

Table 2
Key components and their concentrations for electroless nickel plating solution.

Component	Concentration
$NiSO_4$	30 g·L^{-1}
$Na_3C_6H_5O_7$	25 g·L^{-1}
NaH_2PO_2	20 g·L^{-1}
$NH_3{\cdot}H_2O$	Adjusting pH

Tensile properties of the CFs before and after Ni coating were measured using a fiber strength tester (LLY-06EDC). The stretching speed was 10 mm/min and the initial clamping distance was 10 mm. The fracture strength and the maximum strain were calculated using Eqs. (1) and (2), respectively.

$$\sigma = \frac{F}{A} \tag{1}$$

$$\varepsilon = \frac{\Delta L}{L_0} \tag{2}$$

where σ is fracture strength (GPa); F- tensile strength (CN); A- original cross section of CF (μm^2); ε - elongation at fracture (%); ΔL - elongation (mm); L_0 - original length of CF (mm).

Interfacial bonding strength of the Ni-coated CFs was indirectly characterized by measuring the weight-loss rate of the Ni-coated CFs after an ultrasonic treatment for 30 min. It was calculated using Eq. (3):

$$W\% = \frac{m_1}{m_0} \tag{3}$$

in which W% is weightlessness rate; m_1 (g) is the mass of the Ni-coated CF after ultrasonic treatment; m_0 (g) is the mass of the Ni-coated CF before the ultrasonic treatment. To further determine bonding conditions of the Ni layer on the CFs, Fourier transform infrared (FT-IR) spectra of the CFs after the original adhesive was removed were obtained using a TENSOR 27 spectrophotometer (Bruker, Germany).

Surface wettability is generally characterized by measuring the contact angle of a liquid droplet on the substrate surface, but it is difficult to measure the wetting angles of the CFs owing to their particular shapes. Therefore, we used a dip coating method to verify the improvement of wettability [33]. The CFs, including the untreated and Ni-plated ones, were immersed in a molten tin alloy for a few seconds and then quickly taken out. Their surface morphologies and compositions were characterized using SEM and EDS in order to check their wettability with the liquid metal Sn. Apart from these, we also prepared copper matrix composites by cold-pressing the untreated and Ni-plated CFs, respectively, with a volume fraction of CFs of 5% at a pressure of 400 MPa. The samples were then sintered at 850 °C for 2 h. The interfacial bonding between the CF and copper was characterized to check their wettability.

3. Results and analysis

3.1. Microstructure analysis

Fig. 1 shows SEM images of the CFs before and after coated with a Ni layer. As-received CFs have a smooth surface (Fig. 1(a)). As shown in

Table 1
Specifications and properties of CFs.

Specifications	Number of filament/(number/bunch)	Filament diameter/μm	Tensile strength/GPa	Elastic modulus/GPa	Density/g·cm^{-3}	Elongation at break/%
T700	12 K	7	3.9	241	1.80	1.97

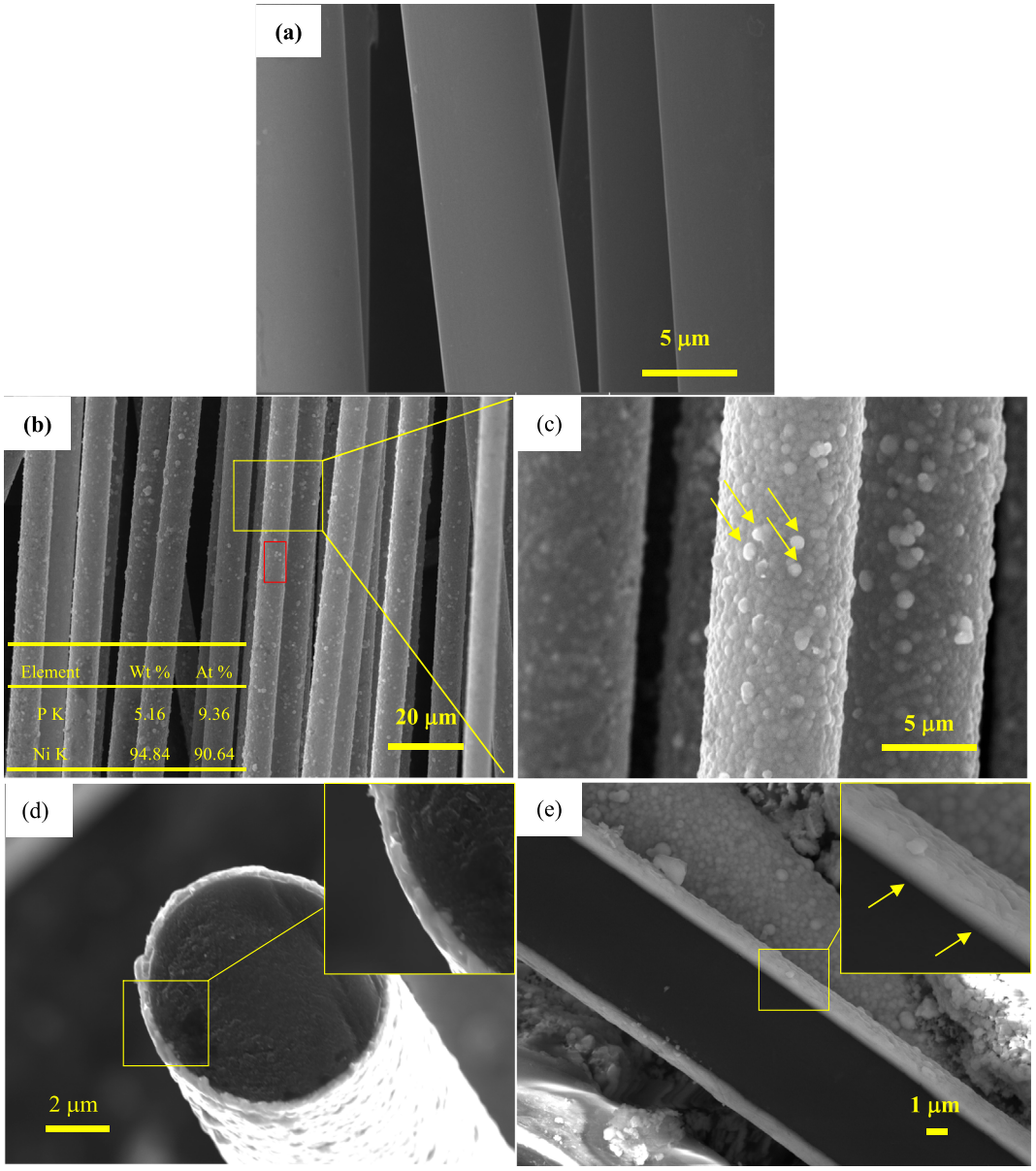

Fig. 1. SEM images of CFs: (a) as-received CFs; (b) Ni-coated CFs (the inset lists the EDS result of Ni-coated CFs); (c) high magnification image of the selected area in (b); (d) cross-section image of Ni-coated CF; (e) axial cross-section image of Ni-coated CF.

Fig. 1(b), the surface of CFs was deposited with the Ni layer which is continuous and homogeneous. According to the EDS results (Fig. 1(b), the surface of CFs was successfully coated with nickel and a tiny amount of phosphorous. In Fig. 1(c), the coating shows many nickel particles on its surface [34–37], and some small white dots (Fig. 1(c)) also appear on the coating, and they have the same compositions as those of the nickel particles. Based on the characterization results, it is assumed that during deposition the nickel ions were adsorbed onto the surfaces of CFs and then were strongly reduced in alkaline conditions to form metal particles. Meanwhile a small amount of phosphorus atoms were also formed in the Ni layer by the electroless deposition method [31,32]. The chemical reactions during the deposition process are written in Eqs. (4)–(7) [38]:

$$H_2PO_2^- + H_2O \rightarrow HPO_3^{2-} + H^+ + 2[H] \quad (4)$$

$$Ni^{2+} + 2[H] \rightarrow Ni^0 + 2H^+ \quad (5)$$

$$H_2PO_2 + H_2O \rightarrow H[HPO_3]^- + H_2 \quad (6)$$

$$H_2PO_2^- + H_2O \rightarrow H[HPO_3]^- + H_2 \quad (7)$$

The cross-section morphology of the nickel coated CFs is shown in Fig. 1(d), which reveals that the CF surface is uniformly coated with a layer of metallic Ni along the circumference of the fiber, and the layer thickness is ~0.5 μm. The Ni layer is distributed uniformly and continuously along the length direction of the fiber, and the interfaces between adjacent particles can be clearly observed as shown in Fig. 1(e).

The XRD result of the Ni-coated CFs is shown in Fig. 2(a). There are three dominant diffraction peaks, corresponding to three face-centered cubic nickel crystal orientations of (111), (200) and (220), respectively. The characteristic peak corresponding to the (002) crystal plane of graphite was found to be at $2\theta = 25^\circ$, and the corresponding peak of the coated CFs is much weaker when compared with that of the uncoated CFs (Fig. 2(b)). XRD analysis clearly indicates that nickel was successfully coated onto the surfaces of the CFs [31].

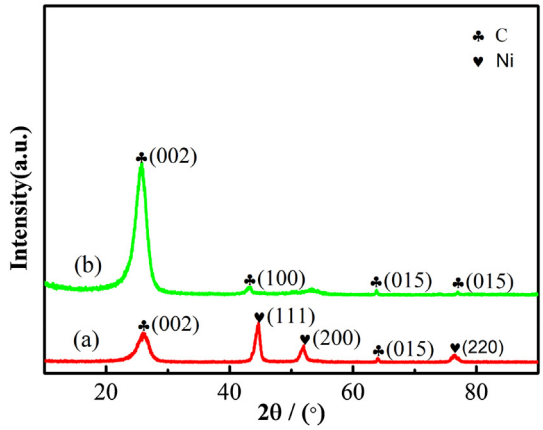

Fig. 2. XRD spectra of (a) Ni-coated CFs and (b) uncoated CFs.

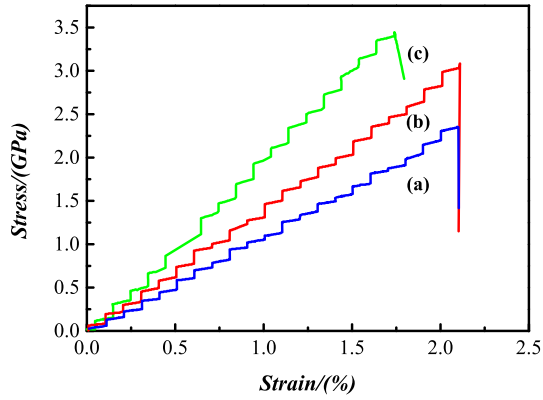

Fig. 3. Tensile testing results of CFs after different treatments: (a) Ni-coated; (b) surface-treated; (c) removal of adhesive.

3.2. Mechanical properties

Fig. 3 shows stress vs strain curve of the CFs after different treatments. All the CFs showed brittle fracture behaviors and were broken right after the elastic deformation. The fracture strength of CFs was decreased after their surfaces have been chemically treated and then coated with a Ni layer.

Tensile testing results of all the CFs are summarized in Table 3. Compared with that of the as-received CFs (Table 1), the fracture strength of CFs after removal of adhesive is 3.5 GPa and the elongation at break is 1.67%. Fracture strength of the CFs after the chemical treatment was reduced to 3.06 GPa, whereas its maximum strain was increased to 1.94%. The fracture strength of the Ni-coated CFs was reduced to 2.25 GPa (e.g., a 35.7% decrease), and the maximum strain was increased to 2.06% (e.g., a 23.4% increase).

There are four factors that cause the decrease of fracture strength:

(1) The high temperature oxidation process during the adhesive removal process causes surface damages of the CFs. The bonding strength between the CF and nickel layer is closely related to the pre-treatment process [39]. Increasing surface roughness of the CFs is an effective method, but it easily produces defects on the surface of the CFs. These defects will cause stress concentration, thus resulting in the decrease of tensile properties of the CFs.
(2) According to the XRD results, residual tensile stress exists in the coated Ni layer. The residual stress in the fiber was obtained using the 2θ-sin^2(ψ) method, and the results are shown in Fig. 4. The measured stress is 42.9 MPa, tensile. Under the combined actions of residual tensile stress and external normal load, the fracture of CFs is accelerated and the tensile strength is reduced.
(3) Because of the huge difference in the mechanical properties between Ni and CFs, the deformation of the Ni layer is incompatible with that of the CFs during the stretching process (Fig. 5). This produces a stress concentration and micro-cracks are formed at their interfaces, which will affect the bonding between the Ni layer and CFs and thus accelerate the earlier fracture of the CFs [30,40].
(4) Tensile properties of metal coated CFs are directly linked with the type of coating material, quality of the coating (including layer thickness, continuity, uniformity and impurity), coating process and parameters [41–46]. When the strengthening effect generated by the Ni coating process is not as significant as the negative influences of newly generated defects caused by the pre-treatment processes, the mechanical properties of the Ni coated CF will be degraded. With the increase of thickness of metal layer, the strengthening effect of the Ni coating will be reduced, not only due to the generation of more defects in the surface layer [40], but also due to the lower tensile strength of nickel (345 MPa) compared with that of CFs (3.9 GPa) [42].

Table 3
Tensile test results of the CFs after different treatments.

Samples	Maximum strain/%	Fracture strength/GPa
CFs after removal of adhesive	1.67	3.50
Surface-treated CFs	1.94	3.06
Ni-coated CFs	2.06	2.25

In Ref. [19], $Ni(CO)_4$ was used as a precursor to deposit a continuous nickel layer on the CFs based on MOCVD, but an enhanced fracture strength of the CFs after coated with Ni layer was reported in that reference, which is different from this study. The possible difference could be that the fine nano-size nickel particles can be filled into those defects such as cracks and voids in the CFs, which can effectively delay the initial fracture of the fiber, thus the fracture strength of the CFs was improved in their study.

Although in this work, the Ni coating causes a slight decrease of tensile strength of the CFs, for the CF reinforced metal matrix composites, this might not be a critical problem for their practical applications. The general failure modes of fiber reinforced composites include pulling-out, stripping and breaking of CFs from the metal matrix. These are mainly due to interfacial wetting and bonding problems, which will be studied in following sections.

3.3. Fracture morphology

Fig. 6 shows the fracture morphologies of the uncoated and Ni-coated CFs, which is quite rough with irregular granular structures (Fig. 6(a)); whereas that of the Ni-coated CFs shows more lamellar structures, mainly distributed in the core of the granular structures (Fig. 6(b)). It can be seen from Fig. 6(b) that the nickel layer has a good adhesion with the CFs after breaking of the fiber.

FT-IR spectra of the chemically treated and adhesive-removed CFs are shown in Fig. 7. The spectrum of the adhesive removed CFs in Fig. 7(b) shows the existence of many peaks: e.g., absorption peak due to the −O−H stretching vibration of hydroxyl groups at 3450 cm^{-1}; the −C═O stretching mode at 1650 cm^{-1}; the vibration mode of −C−O at 1450 cm^{-1}; and the −C−O−C stretching vibration at 1120 cm^{-1}. The intensities of all the peaks which are correlated to the oxygen functional groups of chemically treated CFs are increased dramatically if comparing Fig. 7(a) with Fig. 7(b). Based on the appearance of more oxygen functional groups on the surfaces of the treated CFs measured from the FT-IR, we can conclude that the chemical reactivity of the treated CFs has been improved.

After the ultrasonic treatment of Ni-coated CFs at room temperature (25 °C) for 30 min, the Ni layer did not peel off and the solution did not

psi-Angle	phi	sin(psi)^2	2-Theta	d(?)	%(d-d0)/d0	Shape	Skew	FWHM
☑ 0.0	0	0.000	106.077 (0.007)	1.4328 (0.0001)	---	0.134v	-0.059	0.956 (0.006)
☑ 15.0	0	0.067	106.101 (0.012)	1.4326 (0.0002)	-0.015(0.018)	0.164v	0.040	0.928 (0.010)
☑ 30.0	0	0.250	106.105 (0.013)	1.4325 (0.0002)	-0.018(0.019)	0.214v	0.007	0.838 (0.012)

* Compressive Stress = 42.94 (37.34) MPa [E=68.9x10^3, v=0.345], R=1.000, Profile Fit = pseudo-Voigt

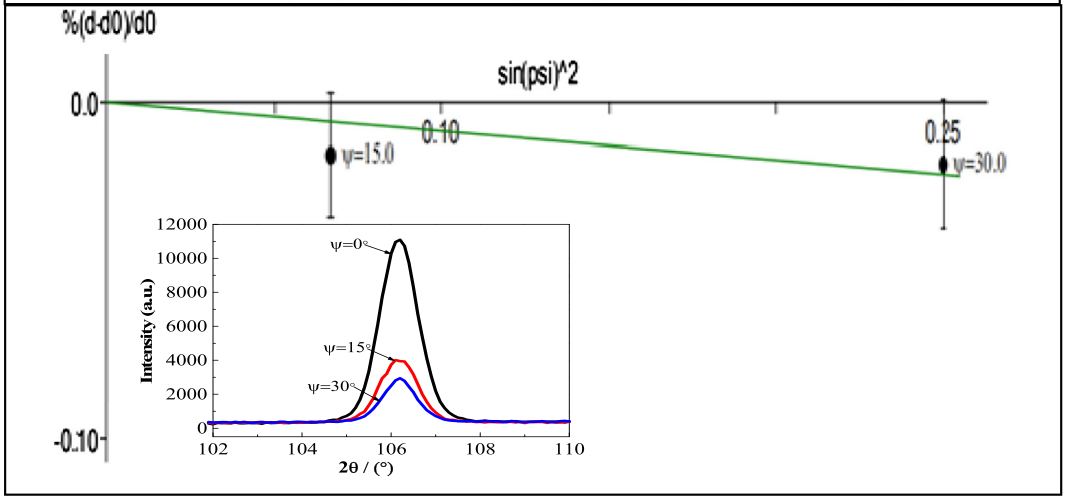

Fig. 4. Residual stress in the nickel coated CFs which was obtained using the 2θ-sin^2(ψ) method from XRD test.

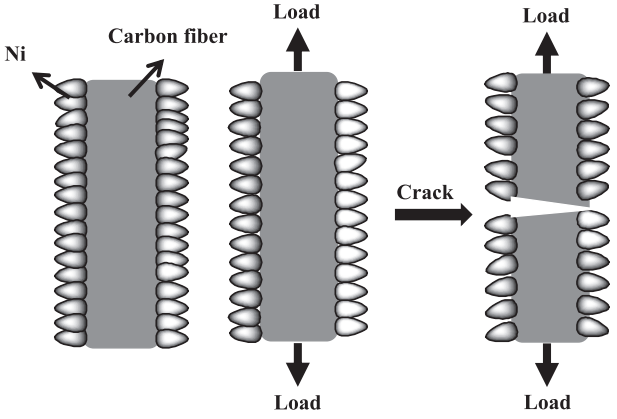

Fig. 5. Schematic illustrations of failure mechanisms for the Ni-coated CFs.

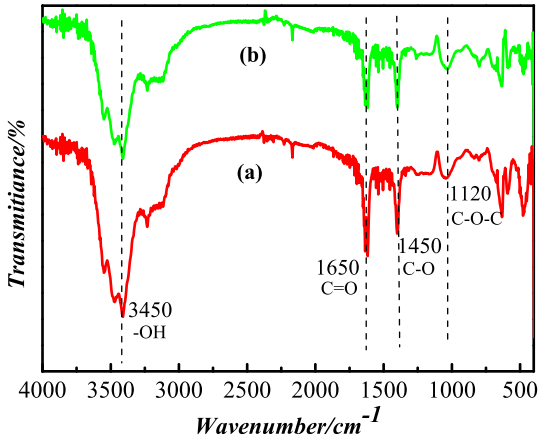

Fig. 7. FT-IR spectra of (a) roughed surface of CFs and (b) CFs with adhesive removed.

show apparent changes. The weight loss rate of the Ni-coated CFs was measured to be 5.8%. There are large Ni particles on the surfaces of CFs (Fig. 1(c)). If the adhesion of the Ni layer is poor, during the ultrasonic process, the particles are easily detached, and the weight loss will be increased significantly. After the chemical treatment, oxygen-containing functional groups have been increased on the surfaces of the CFs (evidenced from Fig. 7), and thus the surface reactivity has been increased. The contact areas between the Ni layer and CFs are increased, and the bonding strength is thus increased. The Ni layer electroplated onto the rough surfaces of the treated CFs will have an enhanced interlocking effect, thus increasing the adhesion of the layer to the substrate (which can be proved from the images shown in

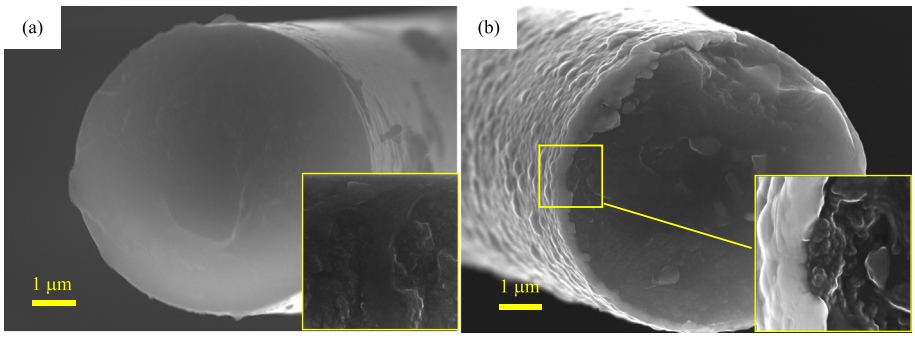

Fig. 6. Fracture morphology of (a) uncoated and (b) Ni-coated CFs.

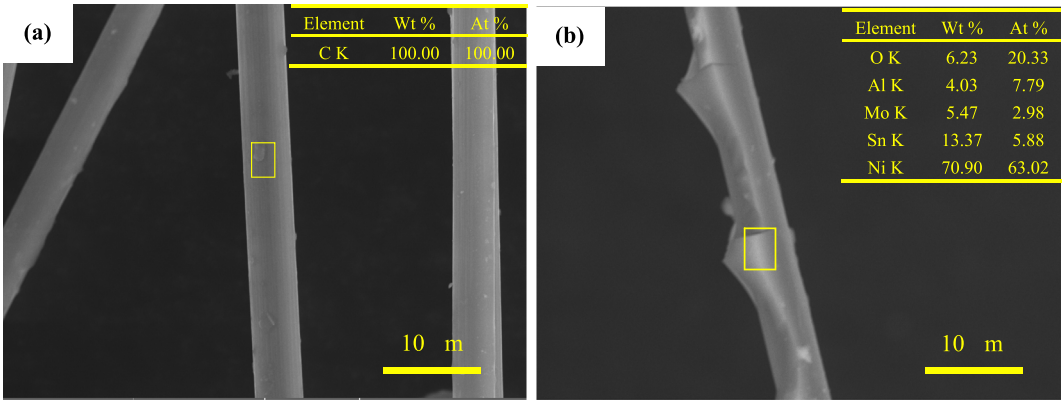

Fig. 8. SEM morphologies and their corresponding EDS analysis results of (a) uncoated and (b) Ni-coated CFs after they have been dip-coated with the molten tin liquid.

Fig. 1(d) and (e).

3.4. Surface wettability

Fig. 8 shows the SEM images of the non-plated and Ni plated CFs after being dip-coated with the molten tin alloys. Fig. 8(a) shows that the non-plated CFs are not adhered well with the tin alloys, which can be verified from the EDS results. However, the adhesion of the Ni-coated CFs to tin alloys has been significantly improved as shown in Fig. 8(b). According to the EDS results, after dip-coating the surface of the Ni-coated CFs has elements of Al, Mo and O, apart from Ni and Sn from the electroplating. The Al and Mo are from the tin alloy, and O is from the surface oxidation during the experiment. The surface tension of the molten tin alloys on the CFs is large and its density is quite different from that of the CFs [47]. During the dip coating process, it is difficult for the CFs to form an effective contact or good adhesion with the molten tin alloys, and the surface of the fiber does not adhere well to the molten tin alloys. When the Ni-coated CFs are immersed in the molten tin alloys, the Ni layer adheres well to the molten tin alloys, and thus the bonding strength is increased significantly. The SEM images in Fig. 8 clearly show that the wettability of the CFs with tin alloys was improved after coated with the Ni layer on their surfaces.

SEM images of the cross-section interfaces between copper matrix and uncoated CFs or Ni-coated CFs are shown in Fig. 9. The interface between the uncoated CF and the copper matrix is clear (Fig. 9(a)), whereas there is a significant metallurgical bonding occurred at the interface between the CF and the copper in the Ni-coated reinforced copper matrix composite material. This further proves that metal-coated CFs can significantly improve the wettability of CFs with the metal.

4. Conclusions

In this paper, we used the electroless plating to coat a layer of Ni onto the CFs to improve the interfacial structures, fracture strain/strength and wettability. Results showed that a Ni layer with a uniform thickness of ~0.5 μm was deposited onto the CFs using an electroless plating method. The CFs were well bonded with the nickel layer and their wettability with the molten Sn alloy and copper matrix composite testing were improved significantly. Compared with the CFs after removal of adhesive, the fracture strength of the Ni-coated CFs was decreased from 3.5 GPa to 2.25 GPa (a 37.5% decrease) and the maximum strain was increased from 1.72% to 2.06% (e.g., a 23.4% increase). The fracture mechanisms of the Ni-coated CFs during tensile tests are summarized as follows: (1) crack generation between the coating layer and fiber due to existence of residual stress and local stress concentration; (2) coating delamination; and (3) brittle fracture of fiber.

Acknowledgement

The authors would like to acknowledge the financial support from Key Research and Development Projects of Shaanxi Province (No. 2017ZDXM-GY-050) and Electrical Materials and Infiltration Key Laboratory of Shaanxi Province Projects (No. 17JS080), Xi'an Science research project of China (No. 2017080CG/RC043), Newton Mobility Grant (IE161019) through Royal Society and the National Natural Science Foundation of China, and Royal academy of Engineering UK-Research Exchange with China and India.

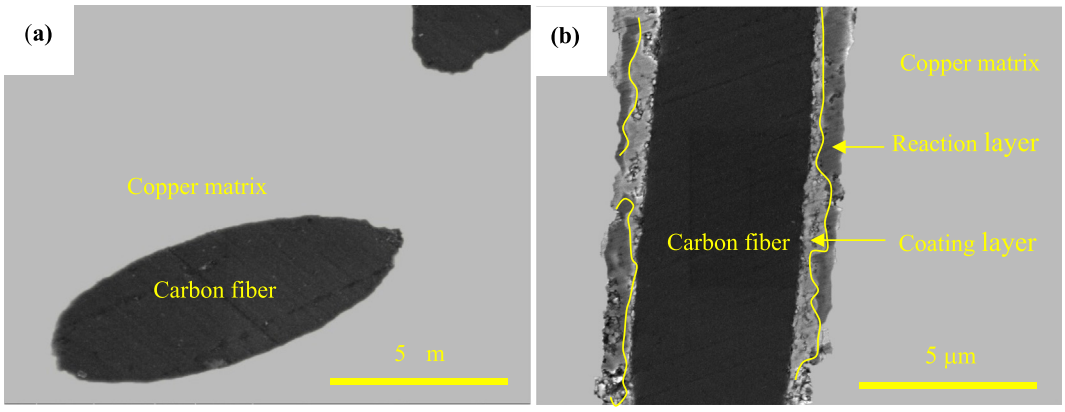

Fig. 9. SEM images of reinforced copper matrix composites prepared using (a) uncoated and (b) Ni-coated CFs.

References

[1] K. Shirvanimoghaddam, S.U. Hamim, M.K. Akbari, S.M. Fakhrhoseini, H. Khayyam, A.H. Pakseresht, E. Ghasali, M. Zabet, K.S. Munir, S. Jia, J.P. Davim, M. Naebe, Carbon fiber reinforced metal matrix composites: fabrication processes and properties, Compos. Part A 92 (2017) 70–96.

[2] B.E. Barton, M.J. Behr, J.T. Patton, E.J. Hukkanen, B.G. Landes, W. Wang, N. Horstman, J.E. Rix, D. Keane, S. Weigand, M. Spalding, C. Derstine, High–modulus low–cost carbon fibers from polyethylene enabled by boron catalyzed graphitization, Small 13 (2017), https://doi.org/10.1002/smll.201701926.

[3] B.A. Newcomb, Processing, structure, and properties of carbon fibers, Compos. Part A 91 (2016) 262–282.

[4] L. Jabbour, D. Chaussy, B. Eyraud, D. Beneventi, Highly conductive graphite/carbon fiber/cellulose composite papers, Compos. Sci. Technol. 72 (2012) 616–623.

[5] S. Li, L. Qi, T. Zhang, J. Zhou, H. Li, Interfacial microstructure and tensile properties of carbon fiber reinforced Mg–Al–RE matrix composites, J. Alloys Compd. 663 (2016) 686–692.

[6] N. Kumar, H.C. Chittappa, S.E. Vannan, Development of aluminium-nickel coated short carbon fiber metal matrix composites, Mater. Today 5 (2018) 11336–11345.

[7] A.T. Miranda, L. Bolzoni, N. Barekar, Y. Huang, J. Shin, S.H. Ko, B.J. McKay, Processing, structure and thermal conductivity correlation in carbon fibre reinforced aluminium metal matrix composites, Mater. Des. 156 (2018) 329–339.

[8] G. Lalet, H. Kurita, T. Miyazaki, A. Kawasaki, J.F. Silvain, Microstructure of a carbon fiber-reinforced aluminum matrix composite fabricated by spark plasma sintering in various pulse conditions, Mater. Lett. 130 (2014) 32–35.

[9] F. Kachold, R. Singer, Mechanical properties of carbon fiber-reinforced aluminum manufactured by high-pressure die casting, J. Mater. Eng. Perform. 25 (2016) 3128–3133.

[10] N.R. Calderon, R. Voytovych, J. Narciso, N. Eustathopoulos, Wetting dynamics versus interfacial reactivity of AlSi alloys on carbon, J. Mater. Sci. 45 (2010) 2150–2156.

[11] J. Zhang, S. Liu, Y. Lu, Y. Dong, T. Li, Fabrication process and bending properties of carbon fibers reinforced Al-alloy matrix composites, J. Mater. Process. Technol. 231 (2016) 366–373.

[12] J. Zhang, S. Liu, Y. Lu, X. Yin, Y. Zhang, T. Li, Liquid rolling of woven carbon fibers reinforced Al5083-matrix composites, Mater. Des. 95 (2016) 89–96.

[13] X.X. Lv, C.X. Lv, Y. Yang, F. An, Y.L. Ji, F. He, Study on nickel plating on carbon fiber, New Chem. Mater. 39 (2011) 89–91.

[14] V. Halouzka, B. Halouzkova, D. Jirovsky, D. Hemzal, P. Ondra, E. Siranidi, A.G. Kontos, P. Falaras, J. Hrbac, Copper nanowire coated carbon fibers as efficient substrates for detecting designer drugs using SERS, Talanta 165 (2017) 384–390.

[15] Y. Wan, T. Cui, J. Xiao, G. Xiong, R. Guo, H. Luo, Engineering carbon fibers with dual coatings of FeCo and CuO towards enhanced microwave absorption properties, J. Alloys Compd. 687 (2016) 334–341.

[16] Y. Wan, J. Xiao, C. Li, G. Xiong, R. Guo, L. Li, M. Han, H. Luo, Microwave absorption properties of FeCo-coated carbon fibers with varying morphologies, J. Magn. Magn. Mater. 399 (2016) 252–259.

[17] K. Osouli, E. Hosseinzade, A. Kianvash, A.A. Entezami, Modified nano-magnetite coated carbon fibers magnetic and microwave properties, Appl. Surf. Sci. 356 (2015) 1086–1095.

[18] W.Q. Zeng, W.M. Zeng, Z.Z. Gao, Y.L. Ma, Electroless nickel-plating on carbon fiber in wire mesh catalyzing method, Surf. Technol. 46 (2017) 276–281.

[19] Y. Li, J.H. Nie, N. Li, X.Q. Liu, C.C. Jia, The preparation and properties of nickel-coated carbon fiber by MOCVD process, J. Funct. Mater. 43 (2012) 1688–1691.

[20] K.A. Dyadyura, K.V. Berladir, P.V. Rudenko, O.A. Budnik, V.A. Sviderskij, Research of properties of composite material based on polytetrafluoroethylene filled with carbon fiber with titanium nanocoating, International Conference on Nanomaterials: Application & Properties, IEEE, 2016(02NSA04-1-02NSA04-4).

[21] P. Baumli, J. Sychev, I. Budai, J.T. Szabo, G. Kaptay, Fabrication of carbon fiber reinforced aluminum matrix composites via a titanium-ion containing flux, Compos. Part A 44 (2013) 47–50.

[22] X.W. Zhao, C.G. Zang, Q.K. Ma, Y.Q. Wen, Q.J. Jiao, Thermal and electrical properties of composites based on (3-mercaptopropyl) trimethoxysilane-and Cu-coated carbon fiber and silicone rubber, J. Mater. Sci. 51 (2016) 1–8.

[23] X.G. Cao, C.L. Liang, S.M. Xia, Preparation and conductivity of carbon fiber coated with silver, Mater. Sci. Forum 847 (2016) 137–142.

[24] Z. Guo, L. Sang, Z. Wang, Q. Chen, L. Yang, Z. Liu, Deposition of copper thin films by plasma enhanced pulsed chemical vapor deposition for metallization of carbon fiber reinforced plastics, Surf. Coat. Technol. 307 ((2016) 1059–1064.

[25] J.A. Garlow, L.K. Barrett, L. Wu, K. Kisslinger, Y. Zhu, J.F. Pulecio, Large-area growth of turbostratic graphene on Ni(111) via physical vapor deposition, Sci. Rep. 6 (2016) 19804.

[26] C. Sun, S. Chen, Z. Li, Controllable synthesis of Fe_2O_3-carbon fiber composites via a facile sol-gel route as anode materials for lithium ion batteries, Appl. Surf. Sci. 427 ((2018) 476–484.

[27] Y. Feng, G.E. Mcguire, O.A. Shenderova, H. Ke, S.L. Burkett, Fabrication of copper/carbon nanotube composite thin films by periodic pulse reverse electroplating using nanodiamond as a dispersing agent, Thin Solid Films 615 (2016) 116–121.

[28] B. Abbasipour, S.M. Monirvaghefi, B. Niroumand, Electroless Ni-P-CNT composite coating on aluminum powder, Met. Mater. Int. 18 (2012) 1015–1021.

[29] V. Vitry, L. Bonin, Formation and characterization of multilayers borohydride and hypophosphite reduced electroless nickel deposits, Electrochim. Acta 243 (2017) 7–17.

[30] J.N. Balaraju, P. Radhakrishnan, V. Ezhilselvi, A.A. Kumar, Z. Chen, K.P. Surendran, Studies on electroless nickel polyalloy coatings over carbon fibers/CFRP composites, Surf. Coat. Technol. 302 (2016) 389–397.

[31] A. Ayta, M. Gürbüz, A.E. Sanli, Electrooxidation of hydrogen peroxide and sodium borohydride on Ni deposited carbon fiber electrode for alkaline fuel cells, Int. J. Hydrog. Energy 36 (16) (2011) 10013–10021.

[32] O.A. Gawad, M.H.A. Tabl, Z.A. Hamid, S.F. Mostafa, Electroplating of chromium and Cr-carbide coating for carbon fiber, Surf. Coat. Technol. 201 (2006) 1357–1362.

[33] D. Kong, X. Zuo, Y. Wang, Y. Zhou, Microstructure and thermal decomposition property of Ni-P/Cr2N composite powder by electroless plating, Adv. Powder Technol. 29 (2018) 1433–1438.

[34] M. Erfanmanesh, R. Shoja-Razavi, H. Abdollah-Pour, H. Mohammadian-Semnani, Influence of using electroless Ni-P coated WC-Co powder on laser cladding of stainless steel, Surf. Coat. Technol. 348 (2018) 41–54.

[35] W. Liu, X.U. Dong-Duo, X.Y. Duan, G.S. Zhao, L.M. Chang, X. Li, Structure and effects of electroless Ni–Sn–P transition layer during acid electroless plating on magnesium alloys, Trans. Nonferrous Metals Soc. China 25 (2015) 1506–1516.

[36] A. Rahman, R. Jayaganthan, Effect of pH values on nanostructured Ni–P films, Appl. Nanosci. 5 (2015) 493–498.

[37] M.L. Bosko, F.A. Marchesini, L.M. Cornaglia, E.E. Miró, Controlled Pd deposition on carbon fibers by electroless plating for the reduction of nitrite in water, Catal. Commun. 16 (1) (2011) 189–193.

[38] P. Sahoo, S.K. Das, Tribology of electroless nickel coatings – a review, Mater. Des. 32 (4) (2011) 1760–1775.

[39] J.J. Zhang, S.C. Liu, H. Chen, Y.P. Lu, Q.S. Chen, Y. Dong, T. Wang, Y. Lu, Surface pretreatment and fabrication technology of woven carbon fiber cloth aluminium alloy matrix composite, Mater. Sci. Forum 816 (2015) 3–8.

[40] E. Hajjari, M. Divandari, A.R. Mirhabibi, The study of electroless coating of nickel on carbon fibers, Iran. J. Mater. Sci. Eng. 1 (2017) 43–48.

[41] C. Shi, J. Lei, S. Zhou, X. Dai, L.C. Zhang, Microstructure and mechanical properties of carbon fibers strengthened Ni-based coatings by laser cladding: the effect of carbon fiber contents, J. Alloys Compd. 744 (2018) 146–155.

[42] N.I. Baklanova, V.V. Lozanov, N.B. Morozova, A.T. Titov, The effect of heat treatment on the tensile strength of the iridium-coated carbon fiber, Thin Solid Films 578 (2015) 148–155.

[43] Z.J. Dong, X.K. Li, G.M. Yuan, Z.W. Cui, Y. Cong, A. Westwood, Tensile strength, oxidation resistance and wettability of carbon fibers coated with a TiC layer using a molten salt method, Mater. Des. 50 (2013) 156–164.

[44] Y. Zhang, Y. Meng, Y. Shen, W. Chen, H. Cheng, L. Wang, Room-temperature aqueous plasma electrolyzing Al_2O_3 nano-coating on carbon fiber, Appl. Surf. Sci. 419 (2017) 357–364.

[45] M. Das, A.K. Basu, S. Ghatak, A.G. Joshi, Carbothermal synthesis of boron nitride coating on PAN carbon fiber, J. Eur. Ceram. Soc. 29 (2009) 2129–2134.

[46] K.K. Kar, D. Sathiyamoorthy, Influence of process parameters for coating of nickel–phosphorous on carbon fibers, J. Mater. Process. Technol. 209 (2009) 3022–3029.

[47] J. Frostevarg, S. Robertson, V. Benavides, A.V. Soldatov, Embedding carbon fiber structures in metal matrixes for additive manufacturing, Phys. Procedia 89 (2017) 39–48.